Computational Study of Lean Limit Flames in Hydrogen Mixtures to Investigate Flame Propagation Characteristics

Joongoo Jeon [a], Yeon Soo Kim [a], Hoichul Jung [a], Sung Joong Kim[a,b*]
[a] Department of Nuclear Engineering, Hanyang University,
[b]Institute of Nano Science & Technology, Hanyang University
222 Wangsimni-ro, Seongdong-gu, Seoul 04763, Republic of Korea
[*] Corresponding author: sungjkim@hanyang.ac.kr

1. Introduction

The importance of prediction of hydrogen lower flammability limit (LFL) in characterizing fire and explosion hazards has long been recognized in nuclear industry [1]. The LFL is the minimum fuel concentration which can continuously propagate flame. If the hydrogen concentration of the local gas mixture in containment exceeds the LFL, the mixture can combust by ignition. These kinds of combustion are a major threat for containment integrity due to possibility of overpressure. Furthermore, a more detailed risk analysis of the NPP should be performed to verify the potential risk of flame acceleration (FA) and detonation if the concentration exceeds the threshold [2].

Recently, Jeon et al. developed the calculated non-adiabatic flame temperature (CNAFT) model to facilitate prediction of LFL of hydrogen mixture without complex chemical kinetics [3]. The CNAFT model was based on previous model, calculated adiabatic flame temperature (CAFT) model. Although the CAFT model is known for powerful tool for predicting LFL of gaseous mixtures [4], it tends to result in inconsistent accuracy results depending on the mixture conditions. For this reason, the CNAFT model was proposed by analyzing the flame physics based on studies of heat loss mechanisms during upward propagation. The simple model shows the consistent with experimental results for various mixtures including mixtures at elevated initial temperature and with high steam concentration.

Although the model is well established by theoretical derivation on the heat loss rate, it is important to verify the derivation with one-dimensional estimation by more elaborated analysis for flame propagation. In particular, the CNAFT model maintains the concept of threshold peak flame temperature at limiting mixtures as the previous model. The validity of this concept can be identified by numerical analysis of limiting mixtures. Furthermore, The experimentally observed constant flame speed at limiting mixtures also required further identification for more various hydrogen mixtures. Therefore, the objective of this study is to numerically investigate the lean limit flames of hydrogen mixtures to ascertain the confidence of the physical assumptions used in the development of the CNAFT model. The computational domain is the standard tube by Coward and Jones, 1.8 m long with an inside diameter of 5 cm, closed at both ends [5].

2. Physical assumption in calculated non-adiabatic flame temperature (CNAFT) model

The CNAFT can be calculated by the energy conservation equation with considering heat loss mechanism as shown **Equation (1)**. The model can estimate the amount of heat loss according mixture properties based on the heat loss rate from the reaction zone due to conduction into the cooling post-reaction zone. The model reliability was confirmed for H_2-air mixtures up to 300 °C and H_2-air-Steam mixtures up to 40 vol. % steam concentration as shown **Figure 1** [3].

$$\sum n_i \left[\Delta H_{f,i}^0\right]_{reactants} - \sum n_i \left[\Delta H_{f,i}^0 + \bar{c}_{p,i}(T_{CNAFT} - T_{ref})\right]_{products} = Q_{loss} \quad (1)$$
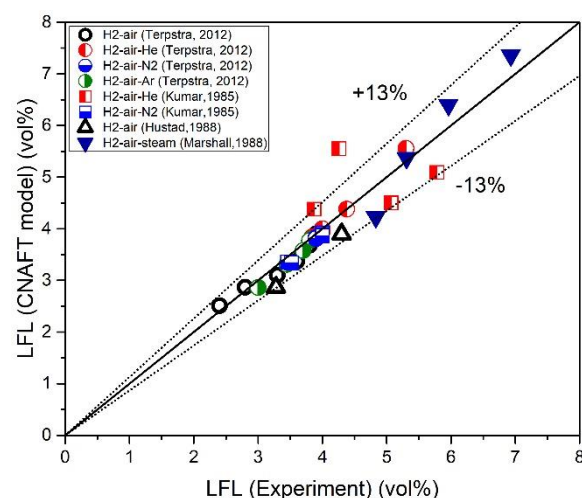
Figure 1. Validation of CAFT model (left) and CNAFT model (right) for various mixtures [3].

The heat loss mechanism basically considered for the prediction of flammability limits are the convective, radiative and conductive heat transfer from the flame to the environment. The radiative heat loss can be classified again as conduction of heat into the post-reaction zone, which is cooled via radiative heat loss $Q_{rad,1}$ and radiative heat loss from the reaction zone itself, $Q_{rad,2}$. It should be noted that Jeon et al. identified that the most of the heat loss determining the peak temperature can be estimated only by regarding the $Q_{rad,1}$ [3]. The vigorous numerical studies for heat transfer mechanism during flame propagation support this conclusion [6, 7]. The conclusion is also consistent with the experimental

observations of Shoshin et al. They pointed out that the reaction zone is effectively cooled by heat conduction to the stagnation zone, which rises upward together with flame and cooled due to radiation heat loss [8].

The CNAFT coefficient, divided thermal diffusivity α by the molar concentration C, can linearly estimate the amount of Q_{loss} as shown **Equation (2)** [3]. ρ_u is the unburnt mixture density, c_p is the isobaric specific heat and k_f is thermal conductivity at flame front. For derivation of the CNAFT coefficient ($\pi = \alpha/C$), two physical assumption each based on previous studies was included. First, the flame speed s_u of the limiting mixtures is independent of the mixture properties and its finite value can be calculated from the results presented by Davies and Taylor [5]. Their observations were derived from experimental results, which proved that an upward propagating flame at the limit of flammability has properties in common with a rising Taylor bubble of hot gas [9]. Second, according to a previously proposed optically thin radiation model, volumetric heat loss rate $R(T_f)$ is determined by the threshold peak temperature and the presence of radiating species. Because the threshold peak temperatures of the limiting mixtures were assumed to be invariable, the volumetric heat loss rate was considered to be constant with the exception of mixtures containing the radiating species. Thus, these two assumptions are based on the theoretical and experimental observations on the heat loss mechanism. However, it is important to verify the assumption by more elaborated numerical analysis for flame propagation. Therefore, we investigated the consistency of flame speed and peak flame temperature at the limiting hydrogen mixtures through CFD analysis.

$$Q_{loss} = k_f \frac{R(T_f)}{\rho_u c_p s_u C} = \frac{\alpha}{C} \frac{R(T_f)}{s_u} \sim \frac{\alpha}{C} \qquad (2)$$

3. Numerical Simulation

3.1 CFD modeling

The CFD simulation was carried by using CHEMKIN-FLUENT code. The two dimensional domain is the standard tube for flammability experiment by Coward and Jones, 1.8 m long with an inside diameter of 5 cm, closed at both ends [5]. Because the flame speed is less than 1 m/s during propagation at limiting mixtures, the laminar flow model was used for the simulation. Gravitation was considered to simulate buoyancy effect due to density difference. In case of chemical kinetics, the so-called San Diego mechanism was solved. It includes 20 reversible elementary reactions among eight reactive species.

Radiation heat flux was calculated using the discrete ordinates (DO) radiation model. It solves the radiative heat transfer for a finite number of discrete solid angle. Since flame thickness at limiting mixtures are very thin, it is close to the optical thin condition. The DO radiation model spans the entire range of optical thickness. A weighted-sum-of-gray-gases model (WSGGM) was used [10]. This model is a compromise between the oversimplified gray gas model and a complete model [11]. The wall boundary condition was treated as a non-slip and iso-thermal condition with each initial temperature. The mesh was uniformly structured to a size of 0.5×0.5 mm, which is similar size of previous CFD study [11]. Soret and Dufour effects was neglected.

3.2 Test matrix

To verify the reliability of CFD simulation, we first simulated the flame propagation of H_2-air mixture at room temperature (Mixture (A) in **Table 1**). The mixture is most frequently used as a benchmark for verification of experimental or computational flammability studies. Next, we analyzed flame propagation in other hydrogen mixtures for our main goal of identifying the consistent of peak temperature and flame speed. As shown **Table 1**, mixture (B) represents the high temperature mixture and mixture (C) represents the mixture containing steam in severe accident conditions. The spark ignition was activated on the bottom of the flame tube at 0 sec.

Table 1. Simulation matrix

Mixture	Composition	X_{steam} (vol.%)	T_i(K)
(A)	H_2-air	0	300
(B)	H_2-air	0	373
(C)	H_2-air-steam	20	400

4. Results and discussions

4.1 Sensitivity analysis of timestep

To observe the flame propagation phenomenon through the tube over time, the CFD simulation was carried out on transient condition. Therefore, It is very important to identify the level of required timestep to ensure the reliability of the results. The most frequently used method for determining the reasonable timestep is the use of the Courant number. The Courant number reflects the portion of a cell that a solute will traverse by advection in one timestep. In our simulation, for unit Courant number, the required timestep was calculated about 2.5e-3 sec. We performed the preliminary simulation to investigate the sensitivity of timestep on simulation results. As similar to expected value, the variation aspect of peak temperature and flame speed converged from the timestep of 2.0e-3. Therefore, the corresponding timestep was used in the flame propagation simulation of our study.

4.2 Verification of CFD simulation

Figure 2 shows the variation of peak temperature and elevation of flame front after bottom ignition. Immediately after ignition, the flame rose at the fastest velocity because the flame peak temperature increased to over 5000 K. However, the peak temperature reduced to

about 1050 K due to a large amount of radiant heat loss. It had a no significant difference from hydrogen-air flame ball at same condition by Fernandez-Tarrazo [12]. After that, the peak temperature was kept almost constant because the generated heat by chemical reaction transferred to both unburned and burned gas. The heat transferred to unburned gas causes another chemical reaction for continuous flame propagation. On the other hand, the heat transferred to burned gas, which is also called post-reaction zone, is considered to be heat loss in terms of flame propagation. The heat loss equation included in the CNAFT model estimates the amount of this heat loss.
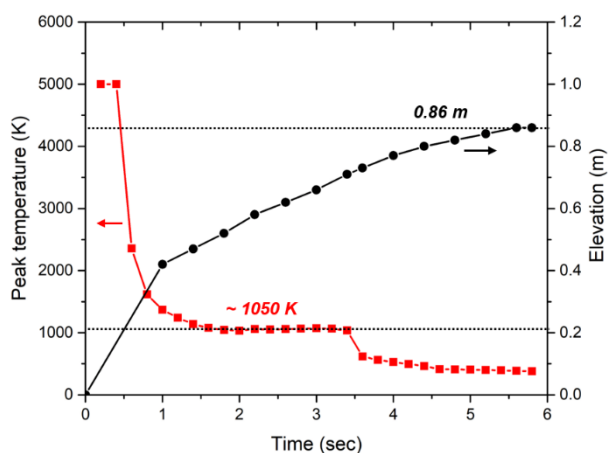
Figure 2. Variation of peak temperature and flame front elevation during propagation in mixture (A)

The saturation of the peak temperature also can be identified in **Figure 3** (upper), which shows the temperature distribution near the reaction zone. **Figure 3** (lower) shows the H distribution to represent the chemical reaction zone. As flame propagates upward, the unburned mixture enters reaction zone past preheating zone. Initially, the bubble-like flames are formed characterized by a long decaying skirt. However, as mentioned before, the reaction zone is effectively cooled by heat conduction to the stagnation zone, which rises upward together with flame and cooled due to radiation heat loss [8]. Therefore, the thickness of flame front becomes gradually and thus the flame shape changes to cap-like flames with a sharp flame edge at the bottom. These observed flame extinction processes are consistent with the experimental results by Zhou [13].

Eventually, the flame cannot maintain the peak temperature (~1050K) from about 3.4 s, and the temperature decrease. Due to the characteristic of lean limit flame raised by buoyancy, a decrease in temperature implies a decrease in flame velocity. The flame gradually decelerated and almost stopped when it reaches 0.86 m. In the standard tube by Coward and Jones, a hydrogen mixture can be considered flammable if the flame propagates more than 1 m. It means that current CFD simulation slightly underestimated the flame propagation distance of the

lean limit flame. Although there are some discrepancy, we concluded that the accuracy of the CFD simulation is reasonable level to predict flame propagation mechanism for other mixtures. This small difference can be caused by the 2D analysis or the model for radiative heat transfer.
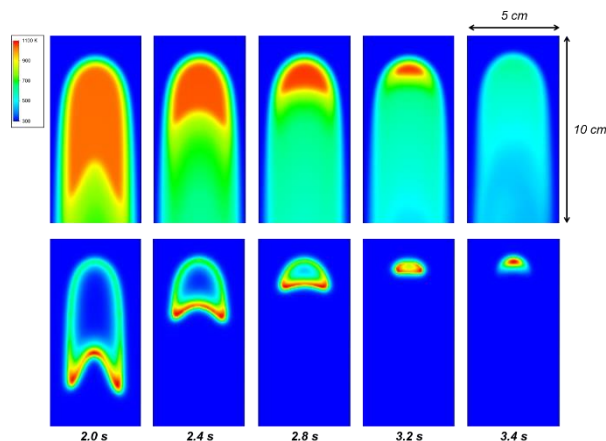
Figure 3. Temperature distribution (upper) and H distribution (lower) in mixture (A)

4.3 Peak temperature and flame velocity

As mentioned, our main goal is identification of the consistent of peak temperature and flame speed independent hydrogen mixture types. For this reason, we compared the variations of the flame propagation in the mixture (A), (B) and (C). **Figure 4** compares the peak temperature changes during flame propagation of each mixture. All mixtures formed a typical flame structure after about 1 s of bottom ignition. They maintained a stable peak temperature until the extinction in about 3.4 s. The peak temperature at stable region was almost same for mixture (A) and (B). It means that high initial temperature has negligible effect on the amount of peak temperature. In case of Mixture (C), which contains 20 vol.% steam, maintained the stable region a little longer. The value of stable peak temperature was about 1130K, 7% relative difference to other mixtures. Further studies have been needed to investigate the peak temperature when the steam concentration more increases.

On the other hand, **Figure 5** compares the elevation of flame front flame propagation of each mixture. It should be noted that the flame velocity was almost constant in the stable peak temperature region. The averaged flame velocity in this region was compared by normalization based on the mixture (A) like the inside graph. Similar to the peak temperature comparison, mixture (B) had almost same average velocity with (A) and mixture (C) had a relative difference about 10%. These results demonstrated the validity of the assumption in the CNAFT model that the flame speed of the limiting mixtures is independent of the mixture conditions [5]. As Liao announced, for low viscosity and high surface tension systems in a sufficiently large diameter, the gas velocity only depends on the geometric

parameter [14]. Although the more simulation to investigate the various limiting mixtures was required, these results thoroughly support the CNAFT model assumption. These further simulations are our future works.
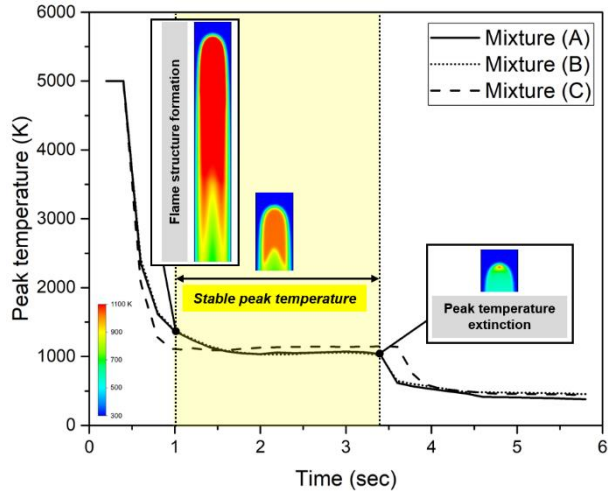
Figure 4. Variation of peak temperature in mixture (A), (B), (C)
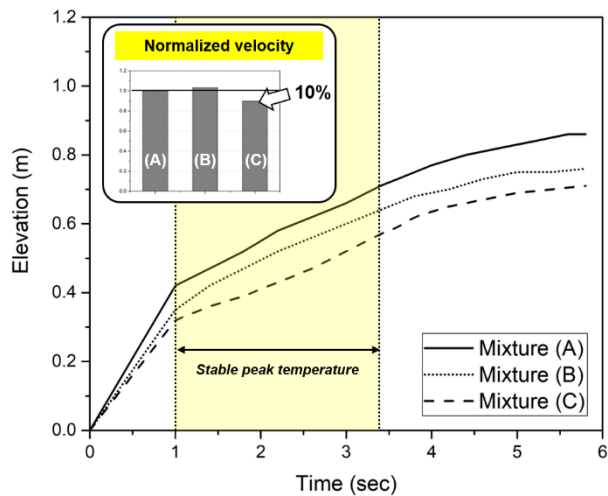
Figure 5. Variation of flame front elevation in mixture (A), (B), (C)

5. Conclusions

In this study, we numerically investigated the lean limit flames of hydrogen mixtures propagating a tube in an upward flow. As the flame became extinct, the flame shape changed to cap-like flames with a sharp flame edge at the bottom from bubble-like flames characterized by a long decaying skirt We identified that, as the CNAFT model assumes, the flame propagation speed through the tube was almost constant for lean limit flames. The peak flame temperature was also found to be insensitive to the limit mixture type even for H_2-air-steam mixture. Although the more simulation to investigate the

consistence of flame speed and peak temperature for various limiting mixtures has been required, these results will contribute to the CNAFT model to gain more confidence in the hydrogen hazard analysis. These further simulations and verifications are our future works. Also more analysis should be carried out for local flame physics such as instability and flame stretch effect.

REFERENCES

1. A. Bentaib, N. Meynet, A. Bleyer, Overview on hydrogen risk research and development activities: methodology and open issues, Nucl. Eng. Technol. 47 (2015) 26-32.
2. N.K. Kim, J. Jeon, W. Choi, S.J. Kim, Systematic hydrogen risk analysis of OPR1000 containment before RPV failure under station blackout scenario, Ann. Nucl. Energy 116 (2018) 429–438.
3. J. Jeon, W, Choi, S.J. Kim , A flammabiltiy limit model for hydrogen-air-diluent mixutres based on heat transfer characteristics in flame propagation, Nucl. Eng. Technol., revision.
4. M. Vidal, W. Wong, W.J. Rogers, M.S. Mannan, Evaluation of lower flammability limits of fuel–air–diluent mixtures using calculated adiabatic flame temperatures, J. Hazard. Mater. 130 (2006) 21–27.
5. H.F. Coward, G.W. Jones, Limits of flammability of gaseffyels and vapors, US Bureau of Mines, 1957, Bulletin 627, Pittsburgh, Pennsylvania, USA.
6. K.P. Lakshmisha, P. Paul, H. Mukunda, On the flammability limit and heat loss in flames with detailed chemistry, Proc. Combust. Inst. 23 (1991) 433–440.
7. H-J. Liaw, K-Y. Chen, A model for predicting temperature effect on flammability limits, Fuel 178 (2016) 179-187.
8. Y. Shoshin, J. Jarosinski, On extinction mechanism of lean limit methane-air flame in a standard flammability tube, Proc. Combust. Inst. 32 (2009) 1043–1050.
9. A. Levy, An optical study of flacmmability limits, Proc. R. Soc. Lond. A. 283 (1965) 134–145.
10. A. Coppalle, P. Vervisch, The total emissivities of high-temperature flames, Combust. Flame   49 (1983) 101-108
11. Y. Shoshin, L. Tecce, J. Jarosinski, Experimental and computational study of lean limit methane-air flame propagating upward in a 24 mm diameter tube, Combust. Sci. Technol. 180 (2008) 1812-1828.
12. E. Fernandez-Tarrazo, A.L. Sanchez, A. Linan, F.A. Williams, The structure of lean hydrogen-air flame balls, Proc. Combust, Inst. 33 (2010) 1203-1210.
13. Z. Zhou, Y. Shoshin, et al., Experimental and numerical study of cap-like lean limit flames in H2-CH4-air mixture, Combust. Flame 189 (2018) 212-224.
14. Q. Liao, T.S. Zhao, Modeling of taylor bubble rising in a vertical mini noncircular channel filled with a stagnant liquid, Int. J. Multiphase Flow 29 (2003) 411-434.